Available online at www.sciencedirect.com
ScienceDirect
Trans. Nonferrous Met. Soc. China 34(2024) 1694−1709
Transactions of Nonferrous Metals Society of China
www.tnmsc.cn

Variations in structure and adsorption characteristics of humic acid during pressure oxidation process

Hui-qun NIU[1,2], Rong-xin ZHAO[3], Hong-ying YANG[1,2], Lin-lin TONG[1,2], You-qin ZHOU[2,4]

1. Key Laboratory for Ecological Metallurgy of Multimetallic Mineral (Ministry of Education), Northeastern University, Shenyang 110819, China;
2. School of Metallurgy, Northeastern University, Shenyang 110819, China;
3. Jiaojia Gold Mine, Shandong Gold Group Co., Ltd., Laizhou 264100, China;
4. Joe Zhou Mineralogy Ltd., Peterborough, Ontario K9L 2A6, Canada

Received 4 October 2022; accepted 23 March 2023

Abstract: Humic acid extraction from carbonaceous pressure-oxidized gold ore was carried out. The structure of humic acid was analyzed utilizing elemental analysis, FTIR, UV−Vis, Raman spectra and XPS. Also, the kinetic and isotherm models of the gold-adsorbing process were established to calculate the thermodynamic parameters and isosteric heat of adsorption. The results showed that affected by pressure oxidation, the aliphatic structure, C═O and other oxygen-containing groups were destroyed. Most importantly, new bonds, such as C—O—Cl_x, C—Cl_x and Me_4N—Cl, were formed in the humic acid extracted from pressure-oxidized gold ore. The adsorption test results showed that, pressure oxidation made a profound impact on the gold-adsorbing performance of humic acid. The adsorption rate of humic acid decreased to (42.78±1.05)% for the pure gold solution and (28.63±1.11)% for the gold leaching solution after pressure oxidation. Adsorption findings conformed to the pseudo-second-order and Langmuir isotherm models. The isosteric adsorption heat of humic acid increased with the increase of the adsorption amount.
Key words: humic acid; orthogonal experiment; pressure oxidation; structural change; adsorption behavior

1 Introduction

Carbonaceous gold ores are widely distributed, mainly in the United States, South Africa and the China's "Golden Triangle" region, with huge reserves [1]. However, carbonaceous gold ores are one of the most complex types and are challenging to utilize. The main reasons for this matter are two aspects: one is the gold encapsulated by pyrite and arsenopyrite in microscopic or submicroscopic forms, the other is the presence of carbonaceous matters severely interfering with the gold leaching, further triggering the "preg-robbing" effect [2,3]. Carbonaceous gold ores have a complex and diverse mineral composition and contain various carbonaceous matters. Studies have shown that carbonaceous matters lead to the "preg-robbing" phenomenon when the content in a gold ore exceeds 0.2% [4]. Carbonaceous matters are mainly composed of elemental carbon, humic substances and hydrocarbons [5]. Elemental carbon can be found in almost any carbonaceous gold ore, and yet hydrocarbons are uncommon [6]. Humic substances can be divided into three parts according to solubility: humic acid, fulvic acid and humin [7,8]. Humic acid is the most common and essential component of humic substances. Humic acid particles generally occur as a black or dark brown powder with fine particle size. Humic acid exhibits

Corresponding author: Hong-ying YANG, E-mail: yanghy@smm.neu.edu.cn
DOI: 10.1016/S1003-6326(24)66500-3

chemical activity and contains a variety of chemical groups, such as carboxyl, phenolic and alcoholic hydroxyl groups, carbonyl groups and other oxygenated structures [9,10]. Furthermore, it is a macromolecular organic acid structure containing benzene rings, polycyclic aromatic hydrocarbons and aliphatic chains [11]. Humic acid was found to possess ion exchange, complexation and redox capabilities [12]. Our previous study showed that the gold adsorption behavior of humic acid was mainly dominated by chemisorption, accompanied by gold reduction [13].

The related study reported that the interference of carbonaceous matters with gold was carried out through adsorption, specifically surface-active site adsorption (pores, defects and carbon edges), ion exchange, complexation to form a stable gold-organic cyclic compound and chemical reduction [4]. Thus, eliminating or shielding carbonaceous matters is the key to treating this type of gold ore. The generally employed and processing-matured pretreatment techniques for refractory carbonaceous gold ores include oxidative roasting, pressure oxidation, biological oxidation and chemical oxidation [6,14−16]. Especially, in numerous domestic and foreign gold enterprises, pressure oxidation technology was applied. Furthermore, a mass of experimental and industrial data support the efficacy in the treatment of refractory carbonaceous gold ores [17,18]. Pressure oxidation can destroy the sulfides and cause gold exposure while oxidizing and decomposing inorganic carbon and organic carbon. However, according to our previous research [19], pressure oxidation had a relatively limited ability to decompose organic carbon, and yet it was more likely to destroy the chemical structure or inhibit the surface activity, thus passivating the organic carbon surface and reducing the gold-adsorbing capability [20]. As a result, what is the form of structural change of humic acid affected by pressure oxidation? What does the gold-adsorbing performance of the structurally changed humic acid vary? There are no relevant studies giving analysis and conclusions. Thus, this research will fill the work gap in this field.

Through an in-depth study, the main objectives of this work are to reveal the structural changes of humic acid affected by pressure oxidation and to dissect the gold-adsorbing process. These will provide theoretical guidance and research significance on the pressure oxidation degradation theory of carbonaceous matters for the future. Additionally, this study provides an in-depth analysis of the structural variations and gold-adsorbing capacity of humic acid treated by pressure oxidation from the mechanism, aiming at improving the basic theory, technical operation parameters and process indexes.

2 Experimental

2.1 Materials

2.1.1 Refractory carbonaceous pressure-oxidized ore

The refractory carbonaceous pressure-oxidized gold ore obtained from Guizhou Province, China, was used to extract humic acid. Table 1 lists the main elemental content in carbonaceous pressure-oxidized gold ore. The XRD pattern of the carbonaceous pressure-oxidized gold ore is shown in Fig. 1. After pressure oxidation, the main metal minerals are iron arsenate, calcium arsenate, jarosite and carphosiderite. Quartz and gypsum are the main gangue.

2.1.2 Humic acid

The extraction of humic acid from refractory carbonaceous pressure-oxidized ore was according

Table 1 Contents of elements in carbonaceous pressure-oxidized gold ore (wt.%)

Au*	Fe	As	S
23.7	9.29	0.611	9.07
Total carbon	**Inorganic carbon**	**Organic carbon**	**Others**
4.08	0.01	4.07	76.949

* g/t

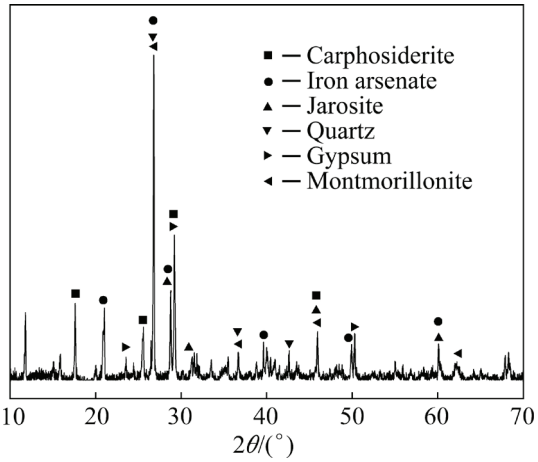

Fig. 1 XRD pattern of carbonaceous pressure-oxidized gold ore

to the method recommended by the International Humic Substances Society (IHSS). NaOH−$Na_4P_2O_7$ mixed solution was used to extract humic acid under specific conditions. After that, the extract was preserved at 25 °C for 1 d and then centrifuged at 3000 r/min for 30 min. The extraction solution was heated at 80 °C for 30 min by a thermostatic water bath, and then conserved at room temperature for 8 h after being acidified with HCl to pH 1−2. The leachate and sediment fractions were separated by centrifuging at 2000 r/min for 10 min. The insoluble particle was humic acid, which was rinsed with deionized water until neutral pH was achieved.

2.2 Gold-adsorbing experiments

The gold-adsorbing experiments involving humic acid were performed in a gold-containing solution under different conditions, and the pH of the solution was adjusted by NaOH or HCl. The amount of humic acid used in the experiments was 20 mg. Each adsorption experiment was conducted in triplicate. After adsorption, the gold-containing solution was filtered and the gold concentration in the filtrate was determined by atomic absorption spectroscopy. The adsorption amount and adsorption rate of humic acid were calculated by using Formulas (1) and (2), respectively [2]. Subsequently, the kinetics and isotherm models were established to describe the gold-adsorbing process. The pseudo-first-order kinetic, the pseudo-second-order kinetic, the Langmuir isotherm and Freundlich isotherm models are displayed in Formulas (3)−(6) [21,22], respectively.

$$q=\frac{(c_0-c_t)V_0}{m} \tag{1}$$

$$\eta=\frac{(c_0-c_t)}{c_0}\times 100\% \tag{2}$$

$$\ln(q_e-q_t)=-k_1t+\ln q_e \tag{3}$$

$$\frac{t}{q_t}=\frac{1}{q_e}t+\frac{1}{k_2q_e^2} \tag{4}$$

$$\frac{c_e}{q_e}=\frac{1}{q_mK_L}+\frac{c_e}{q_m} \tag{5}$$

$$\ln q_e=\ln K_F+\frac{1}{n}\ln c_e \tag{6}$$

where q represents the adsorption amount (mg/g), c_0 is the initial gold concentration (mg/L), c_t is the gold concentration at time t (mg/L), m is the mass of humic acid (g), V_0 is the volume of containing-gold solution (L), η is the adsorption rate (%), q_e is the equilibrium gold adsorption amount (mg/g), q_t is the adsorption amount of gold at time t (mg/g), k_1 is the rate constant of pseudo-first-order kinetics (h^{-1}), k_2 is the rate constant of pseudo-second-order kinetics (mg/(g·h)), c_e is the equilibrium gold concentration (mg/L), q_m is the maximum gold adsorption amount (mg/g), K_L is the Langmuir constant (L/mg), K_F is the Freundlich constant (mg/(g·(mg·L^{-1})$^{1/n}$)), and n is the coefficient of the Freundlich model.

The adsorption thermodynamic parameters, including Gibbs free energy change, enthalpy change, and entropy change, were calculated by the Formulas (7)−(9), respectively [23]. The isosteric heat of adsorption was calculated by using Formula (10) [24], where Q was obtained from the slope of the linear curve under different adsorption amounts.

$$\Delta G=-RT\ln K \tag{7}$$

$$\frac{\partial \lg K}{\partial(1/T)}=-\frac{\Delta H}{2.303R} \tag{8}$$

$$\Delta S=\frac{\Delta H-\Delta G}{T} \tag{9}$$

$$\frac{\mathrm{d}(\ln c_e)}{\mathrm{d}T}=-\frac{Q}{RT^2} \tag{10}$$

where ΔG is the Gibbs free energy change (kJ/mol), K is the equilibrium constant, T is the thermodynamic temperature (K), R is the molar gas constant (8.314 J/(K·mol)), ΔH is the enthalpy change (kJ/mol), ΔS is the entropy change (J/(K·mol)), and Q is the isosteric heat of adsorption (kJ/mol).

2.3 Analytical methods

Elemental analysis was conducted by using an ONH analyzer (ONH836) and an infrared carbon−sulfur analyzer (CS230). The FTIR spectra were recorded over the range between 4000 and 400 cm^{-1} by a Thermo Nicolet−380 spectrometer. UV−Vis spectra were provided on a TU−1901 UV-Vis spectrophotometer between 190 and 800 nm. Further, the second-order derivative of the UV−Vis spectra was performed in the range from 190 to 400 nm. Meanwhile, E_{465}/E_{665} (the ratio of absorbance at 465 nm to that at 665 nm), E_{270}/E_{400} and E_{250}/E_{365} were calculated to characterize the structural properties of humic acid according to the UV−Vis spectra. The defects and preg-robbing capability of humic acid were measured by Raman

spectra (HORIBA LabRAM HR Evolution, λ=633 nm). XPS (Thermo Fisher ESCALAB 250xi) was used to determine the changes in elemental environment of C, H and O by using a K Alpha$^+$ spectrometer with a mono Al K_α source.

2.4 Calculation of extraction amount

The yield of humic acid extracted from carbonaceous pressure-oxidized gold ore samples was determined by potassium dichromate titration method, and the calculation formulas are shown in Formulas (11) and (12) [25]:

$$W_1 = \frac{0.003(V_0 - V_1)C_1}{CG} \times \frac{a}{b} \times 100\% \quad (11)$$

$$W_2 = \frac{W_1}{1 - A} \quad (12)$$

where W_1 is the yield of humic acid (%); W_2 is the yield of dry humic acid (%); V_0 is the volume of $Fe(NH_4)_2(SO_4)_2$ solution consumed in titrating the blank (mL), V_1 is the volume of $Fe(NH_4)_2(SO_4)_2$ solution consumed in titrating humic acid (mL), C_1 is the concentration of standard $Fe(NH_4)_2(SO_4)_2$ solution (mol/L), 0.003 represents the carbon mass equivalent to 1.00 mL $c(Fe^{2+})$=1.0 mol/L $Fe(NH_4)_2(SO_4)_2$ solution (g), a is the total volume of solution (mL), b is the volume in determining (mL), G is the mass of sample (g), C is the value of different types of humic acid, such as weathered coal−humic acid (0.64), lignite−humic acid (0.58), peat−humic acid (0.51) and biomass−humic acid (0.50), and A is the moisture of gold ore sample (%).

The extraction amount of humic acid was calculated based on the proportion of total carbon in the gold ore by using Formula (13), and the amount for per ton of gold ore was obtained by using Formula (14) [19]:

$$A_e = \frac{m_1}{m_0 w_{carbon}} \quad (13)$$

$$G_e = \frac{m_1}{m_0} \times 10^3 \quad (14)$$

where m_0 is the mass of ore used in the extraction process (g), m_1 is the extracted mass of humic acid (mg), w_{carbon} is the mass fraction of total carbon in the pressure-oxidized gold ore, A_e is the extracted amount of humic acid (mg/g), and G_e is the extracted amount of humic acid accounted for per ton of gold ore (g/t).

3 Results and discussion

3.1 Influencing factors of extraction

3.1.1 Orthogonal experimental results

An orthogonal experiment was carried out in the extraction process of humic acid from the pressure-oxidized gold ore. Table 2 presents the experimental conditions and data. As indicated in Table 2, it can be observed that the most critical factor affecting the extraction process is $Na_4P_2O_7$ concentration (Range value=0.2948), followed by temperature, time, NaOH concentration and solid/liquid ratio.

(1) Effect of $Na_4P_2O_7$ concentration

Figure 2(a) shows the effect of $Na_4P_2O_7$ concentration on the extraction. As the concentration of $Na_4P_2O_7$ increased from 0.2 to 0.4 mol/L, the yield of humic acid increased rapidly. This is because the increase in the concentration of $Na_4P_2O_7$ causes the chemical reaction to proceed in the positive direction, as shown in Reaction (15). In addition, Ca^{2+}/Mg^{2+} will be converted into soluble salts. However, when $Na_4P_2O_7$ concentration exceeded 0.4 mol/L, the yield significantly decreased. As the extraction proceeded in the reverse direction, $Na_4P_2O_7$ was hydrolyzed in two different ways, as shown in Reactions (16) and (17), resulting in a decrease in $Na_4P_2O_7$ concentration.

$$R—(COO)_4Ca_2(Mg_2)+Na_4P_2O_7 \rightleftharpoons R—(COONa)_4+Ca_2(Mg_2)P_2O_7 \quad (15)$$

$$P_2O_7^{4-} + H_2O = HP_2O_7^{3-} + OH^- \quad (16)$$

$$P_2O_7^{4-} + H_2O = 2HPO_4^{2-} \quad (17)$$

(2) Effect of NaOH concentration

The effect of NaOH concentration on the extraction is listed in Fig. 2(b). The yield of humic acid increased rapidly as NaOH concentration increased from 0.1 to 0.2 mol/L. This is due to the increase in NaOH concentration triggering to proceed positively, as shown in Reaction (18). However, when NaOH concentration exceeded 0.2 mol/L, the yield of humic acid decreased from (0.6685±0.0009)% to (0.6235±0.0011)%. The increase in Ca^{2+}, Mg^{2+} and OH^- concentrations leads to a rise in calcium hydroxide/magnesium hydroxide concentration, further resulting in the formation of insoluble substances covering the mineral surface.

$$R—(COO)_4Ca_2(Mg_2)+4NaOH \rightleftharpoons R—(COONa)_4+2Ca(Mg)(OH)_2 \quad (18)$$

Table 2 Orthogonal experimental conditions and results of extraction process

No.	Experimental condition					Yield/%
	$c(Na_4P_2O_7)$/(mol·L^{-1})	c(NaOH)/(mol·L^{-1})	Sold/liquid ratio	Temperature/°C	Time/h	
1	0.2	0.1	1:3	60	6	0.4586
2	0.2	0.2	1:4	70	8	0.5277
3	0.2	0.3	1:5	80	10	0.6848
4	0.2	0.4	1:6	90	12	0.7965
5	0.4	0.1	1:3	90	10	0.8820
6	0.4	0.2	1:4	80	12	0.9690
7	0.4	0.3	1:6	60	8	0.6758
8	0.4	0.4	1:5	70	6	0.7349
9	0.6	0.1	1:5	90	8	0.7294
10	0.6	0.2	1:6	80	6	0.7811
11	0.6	0.3	1:3	70	12	0.6732
12	0.6	0.4	1:4	60	10	0.5918
13	0.8	0.1	1:6	70	10	0.5234
14	0.8	0.2	1:5	60	12	0.4761
15	0.8	0.3	1:4	90	6	0.4963
16	0.8	0.4	1:3	80	8	0.5866
I	2.4676	2.5934	2.6004	2.2023	2.4709	
II	3.2617	2.7539	2.5848	2.4592	2.5195	
III	2.7755	2.5301	2.6409	3.0215	2.7690	
IV	2.0824	2.7098	2.7768	2.9559	2.8278	
K_1	0.6169	0.6484	0.6501	0.5506	0.6177	
K_2	0.8154	0.6885	0.6962	0.6148	0.6299	
K_3	0.6939	0.6775	0.6602	0.7554	0.6923	
K_4	0.5206	0.6325	0.6442	0.7390	0.7070	
Range	0.2948	0.0560	0.0480	0.2048	0.0893	

(3) Effect of solid/liquid ratio

As can be seen in Fig. 2(c), when the solid/liquid ratio reduced from 1:3 to 1:4 (in g/mL), the yield of humic acid increased by 7.09%. When the solid/liquid ratio reached 1:4, humic acid existing in the pressure-oxidized ore could fully contact the alkaline-extracted solution and the yield reached (0.6962±0.0007)%. However, when the solid/liquid ratio decreased from 1:4 to 1:6, the yield decreased from (0.6962±0.0007)% to (0.6442±0.0010)%. The higher the concentration of extractant used in the extraction process, the lower the proportion of extractant and the less the chance of collision between humic acid and extraction solution.

(4) Effect of extraction temperature

Figure 2(d) depicts the increase in the yield of humic acid with increasing extraction temperature. The maximum yield of (0.7554±0.0008)% was obtained when the temperature rose to 80 °C. Therefore, increasing the temperature extremely facilitated the extraction of humic acid. However, when the temperature increased from 80 to 90 °C, the yield of humic acid dropped to (0.7390± 0.0007)%. This may be due to the decomposition of sodium pyrophosphate at relatively high temperatures, leading to the formation of disodium hydrogen phosphate.

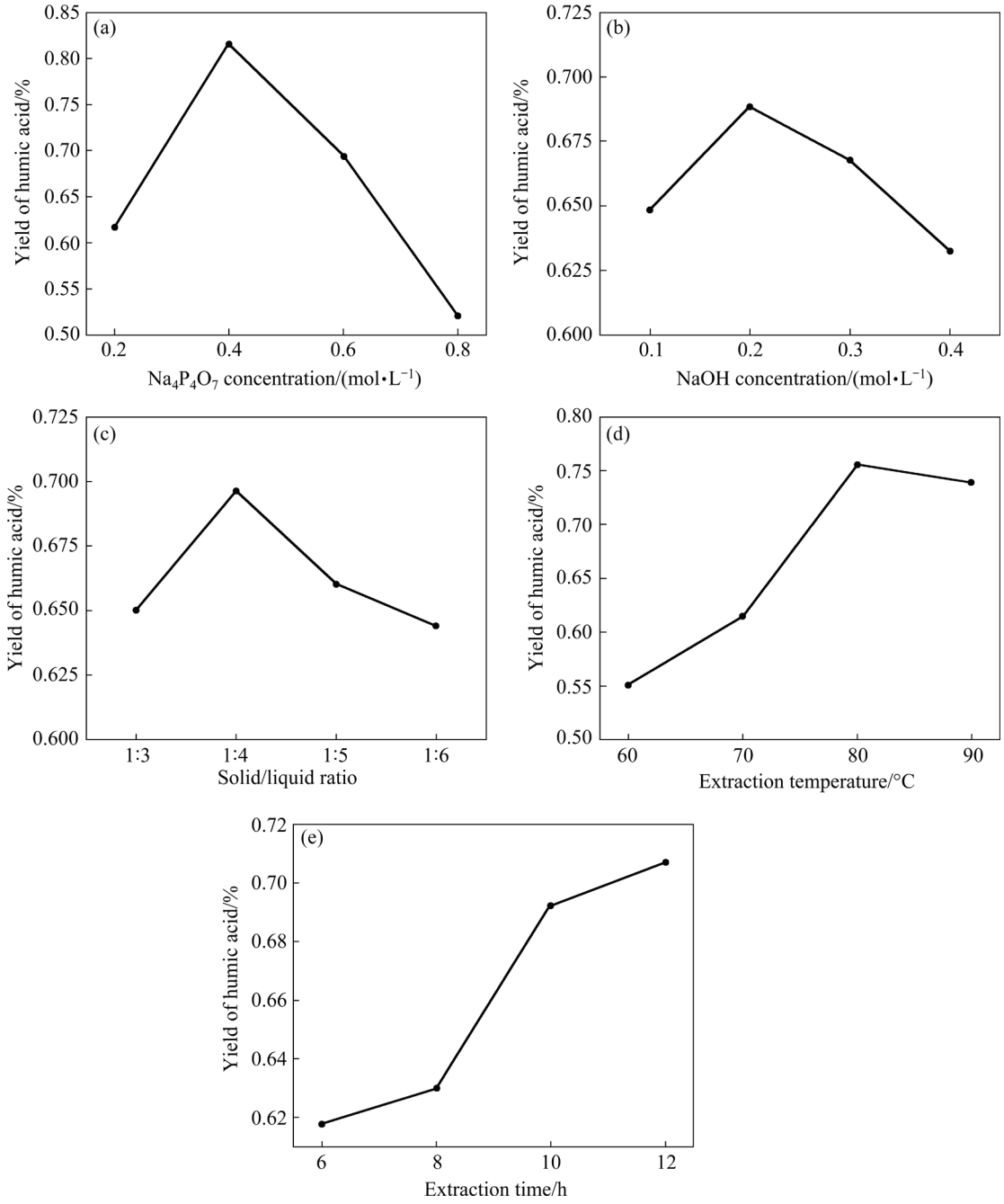

Fig. 2 Influencing factors of extraction process: (a) $Na_4P_2O_7$ concentration; (b) NaOH concentration; (c) Solid/liquid ratio; (d) Extraction temperature; (e) Extraction time

(5) Effect of extraction time

It can be observed from Fig. 2(e) that as the extraction time increases, humic acid can fully contact the substrate of the extraction solution, leading to the insoluble humic acid converting into soluble one. Based on the results in Fig. 2(e), the yield of humic acid increases continuously. However, considering the extraction cost, chemical consumption and the use of the equipment, 12 h was chosen as the optimal extraction time in this work.

3.1.2 Optimal extraction experiment results

The optimal extraction experiments were carried out at $Na_4P_2O_7$ concentration of 0.4 mol/L, NaOH concentration of 0.2 mol/L, solid/liquid ratio of 1:4, extraction temperature of 80 °C and extraction time of 12 h. The optimal extraction experiments were conducted in triplicate. Ultimately, a yield of (0.9704±0.0008)% was obtained.

3.1.3 Extraction amount of humic acid

According to Formulas (13) and (14), the extracted amount of humic acid was 8.26−19.03 mg/g (based on the proportion of total carbon in the ore) and 0.36×10^3−1.29×10^3 g/t (based on the amount accounted for per ton of ore), respectively.

3.2 Structure changes of humic acids affected by pressure oxidation

3.2.1 Elemental analysis results

The content of the main elements of humic acid, including C, H, O and N, was changed under pressure oxidation. The carbon content decreased from 48.69% to 33.31%, and the contents of hydrogen, oxygen and nitrogen decreased from 4.72%, 35.20% and 5.70% to 3.72%, 21.39% and 3.63%, respectively. Table 3 shows the molar ratios of elements in humic acid. The molar ratios of C/N, H/C and O/C are used to describe and analyze the structural features of humic substances. The C/N molar ratio is an important parameter to determine the origin of humic substances [26]. A previous study confirmed that the formation of humic acid might be related to the nonvascular aquatic plant during the long-term geological evolution [19]. In addition, the H/C molar ratio is inversely proportional to the degree of humification/aromaticity [27]. The H/C molar ratio decreased from 1.16 to 0.96 due to pressure oxidation, which implies that the aliphatic structure of humic acid is decomposed, and simultaneously the aromaticity increases. The O/C molar ratio mainly reflects the number of oxygen-containing groups [28]. The O/C molar ratio in Table 3 indicates that humic acid extracted from gold concentrate is higher than that from pressure-oxidized ore, suggesting that the former contains abundant oxygenated structures. Moreover, this entirely shows that pressure oxidation has a decomposed effect on oxygen-containing structures. Therefore, the variations in the molar ratios of elements in humic acid inevitably influence the gold-adsorbing capability.

Table 3 Molar ratios of elements in humic acid

Sample	Molar ratio		
	C/N	H/C	O/C
Humic acid from gold concentrate	9.95	1.16	0.54
Humic acid from pressure-oxidized ore	8.46	0.96	0.48

3.2.2 FTIR spectra

Figure 3(a) shows the FTIR spectra of humic acid. It can be found that the structure of humic acid has changed significantly after pressure oxidation. The absorption peaks caused by the stretching vibration of the C—H bond in —CH_3 and —CH_2— groups [29] disappear. Furthermore, the intensity of an absorption peak at 1385 cm^{-1} related to the symmetric deformation vibration of aliphatic C—H is weakened. These changes fully indicate that pressure oxidation has an intense destructive effect on the aliphatic structure, further leading to the decomposition of carbon or branch chains. In the spectra of humic acid from concentrate, the characteristic absorption peak at 1710 cm^{-1} corresponds to carboxyl, carbonyl or some structure containing C═O [30]. However, the appearance of the absorption peak is not observed in the spectrum of humic acid from pressure-oxidized ore, revealing that the change in C═O structure leads to a decrease in the number of oxygen-containing structures that complex with gold to form gold-organic compounds. The peak at 1120 cm^{-1} is associated with the symmetric C—O stretching vibration of polysaccharides or polysaccharides-like substances [31]. However, the spectrum of humic acid after pressure oxidation shows a shift of the absorption peak toward the long-wave direction (1136 cm^{-1}) and a decrease in peak intensity, which may be due to the variation in the chemical environment of C—O bonds or a decrease in the number of C—O bonds [32]. Moreover, the peak at 933 cm^{-1} attributed to the C—H out-of-plane deformation vibration of the aromatic hydrocarbon disappears after pressure oxidation. On the contrary, affected by pressure oxidation, a stretching vibration peak caused by the hydrocarbon C—O bond [5] appears in the long-wave direction of the spectrum (984 cm^{-1}). The disappearance of COO^- the wagging vibration peak and C—O—C vibration peak (700−400 cm^{-1}) [33] can be found in the spectra.

3.2.3 UV−Vis spectra

Figure 3(b) shows the UV−Vis spectra of humic acid before and after pressure oxidation. Humic acid extracted from gold concentrate and pressure-oxidized ore has a UV absorption peak at 204 and 209 nm, respectively. Both peaks correspond to the alkyl-substituted structure of the benzene ring [34]. This indicates that pressure

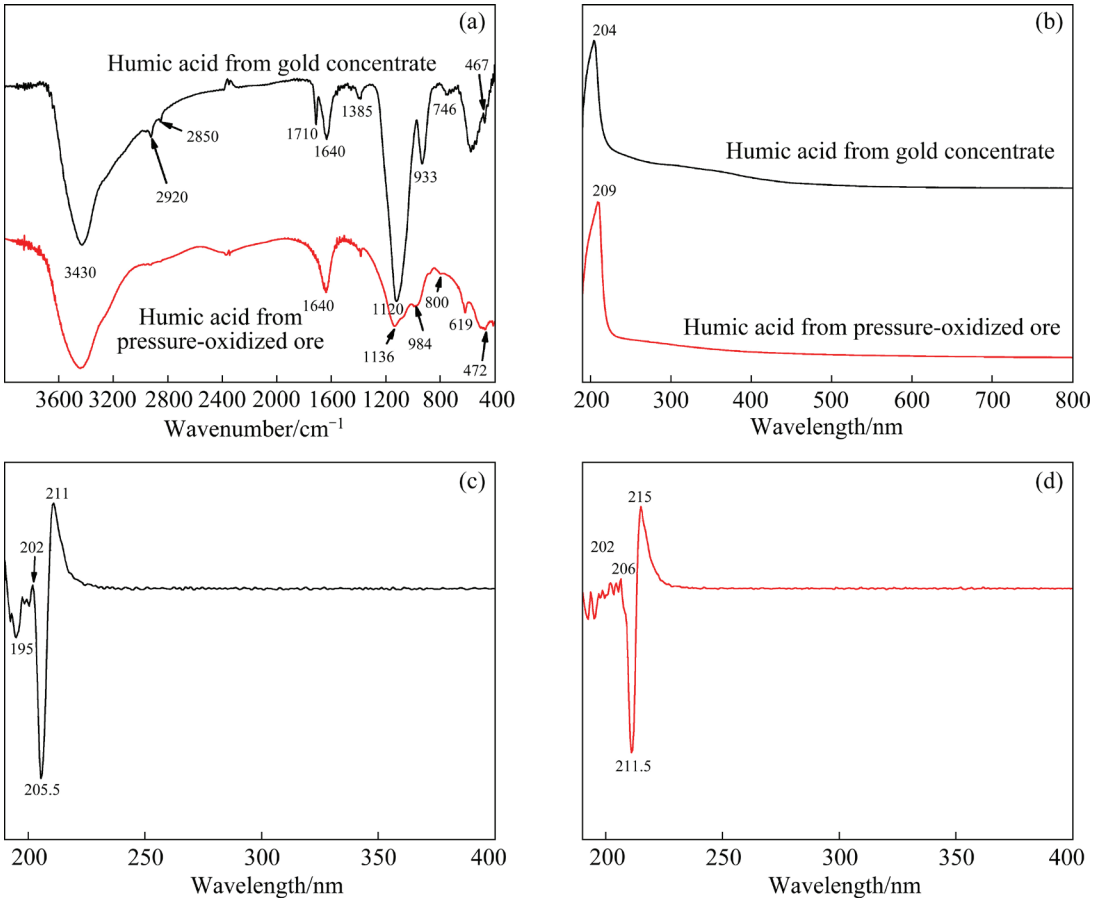

Fig. 3 FTIR (a), UV−Vis (b) spectra of humic acid extracted from gold concentrate and pressure-oxidized ore, and 2DE-UV spectra of humic acid extracted from gold concentrate (c) and pressure-oxidized ore (d)

oxidation does not significantly affect the benzene ring and its substituents. In addition, humic acid has an apparent characteristic absorption in the UV region, but the structural features tend to lead to overlapping peaks. Therefore, performing a second derivative (2DE) for the overlapping absorption peaks is necessary. As shown in Fig. 3(c), four obvious peaks appear at 195, 202, 205.5 and 211 nm, all of which correlate with alkyl-substituted aromatic structures [35]. Similarly, four absorption peaks occurring at 202, 206, 211.5 and 215 nm are observed in Fig. 3(d). The difference in the second derivative spectra indicates that the ultraviolet peaks shift towards the long-wave direction treated by pressure oxidation. This suggests a change in substituent structure or a decrease in the number of alkyl groups.

In the UV−Vis spectra, the absorbance ratios at specific wavelengths provide valuable information on humic acid, mainly including the degree of humification, aromaticity, relative molecular mass and others [36]. The characteristic parameters of humic acid are listed in Table 4. E_{250}/E_{365} is inversely proportional to the relative molecular mass and aromaticity [12]. According to the data, E_{250}/E_{365} value increases from 1.98 to 2.12, showing that pressure oxidation decomposes the aliphatic structure of humic acid. This is also consistent with the results obtained from FTIR spectra. Furthermore, E_{270}/E_{400} value is related to two aspects. One is the chromophore content and the other is the degradation of complex carboxyl/phenol compounds [29]. The ratio of humic acid from pressure-oxidized ore is slightly lower than that from concentrate, which indicates a decrease in chromophores and a weakening degradation trend to simple compounds. Additionally, E_{465}/E_{665} value decreases with increasing humification [37]. The results show that the humification of humic acid decreases under pressure oxidation, which suggests that the aliphatic structures are to be effectively decomposed.

Table 4 UV−Vis characteristic parameters of humic acid

Sample	E_{250}/E_{365}	E_{270}/E_{400}	E_{465}/E_{665}
Humic acid from gold concentrate	1.98	2.42	4.98
Humic acid from pressure-oxidized ore	2.12	2.20	1.87

3.2.4 Raman spectra

Figure 4 presents Raman spectra of humic acid extracted from gold concentrate and pressure-oxidized ore. In the case of carbonaceous matters, the essential characteristic peaks in the Raman spectra are the D and G peaks. Generally, the D peak is associated with lattice order and defects in carbon or deformation vibration of —CH_3 [38]. The in-plane stretching vibration of the carbon atom (sp^2) hybridization and the symmetry/crystallinity of the structure are related to the G peak [39]. Affected by pressure oxidation, the intensity of D and G peaks decreases, which implies that the structure of humic acid is somewhat affected. The intensity ratio of D peak to G peak (I_D/I_G) is usually used to explain the defects in C-atom crystals and sp^2 atomic crystals and is also associated with the gold-adsorbing performance of carbonaceous matters [40]. The higher the I_D/I_G value is, the more the carbon defects are, and the stronger the gold-adsorbing capability is. After calculation, the I_D/I_G value decrease from 2.63 for gold concentrate to 1.43 for pressure-oxidized ore, indicating the decrease in defects of carbon atoms on the humic acid surface and the number of adsorption sites, which lead to a reduction in the gold-adsorbing capacity.

3.2.5 XPS spectra

XPS is a useful analytical tool to analyze the changes in elemental chemical state, valence and chemical environment. XPS survey spectra are shown in Fig. 5. The peaks of the main elements C, O and N can be observed in the XPS survey spectra.

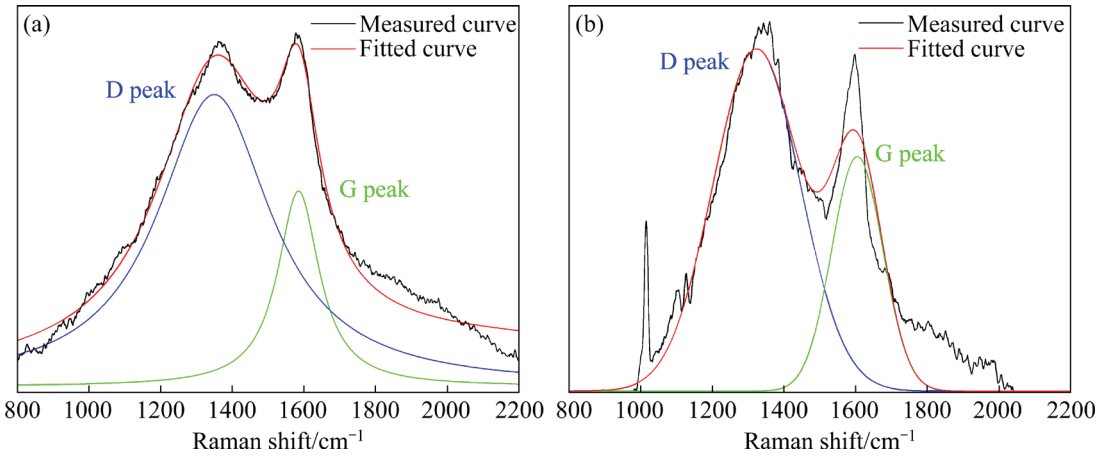

Fig. 4 Raman spectra of humic acid from gold concentrate (a) and pressure-oxidized ore (b)

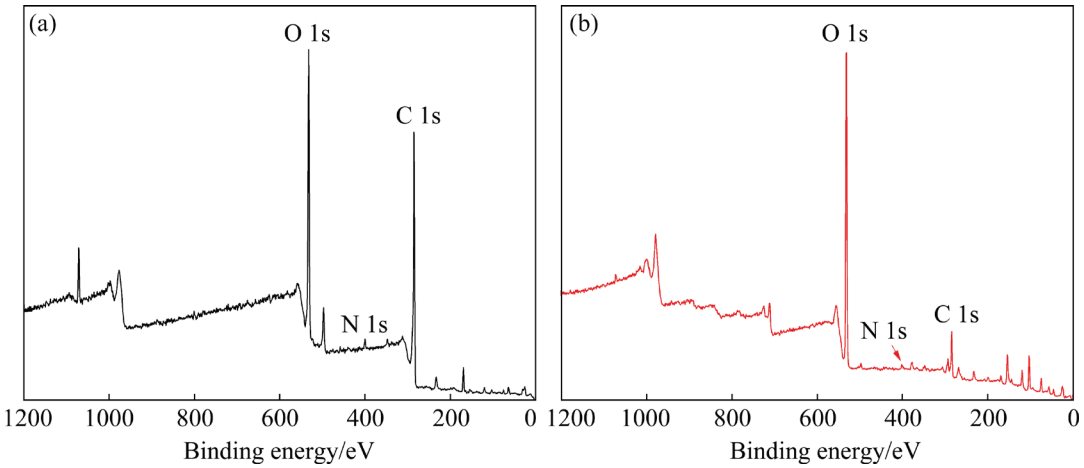

Fig. 5 XPS spectra of humic acid from gold concentrate (a) and pressure-oxidized ore (b)

In order to describe the changes in the chemical environment of these elements, high-resolution narrow-spectra scanning tests were performed for each element. C 1s, O 1s and N 1s spectra are shown in Fig. 6.

Comparing Figs. 6(a) and (b), affected by pressure oxidation, the binding energy of the C—C and O—C═O bonds shifts from 284.25 to 284.6 eV and from 288.52 to 288.9 eV, respectively [41]. The increase in binding energy indicates a variation in the chemical environment of carbon and a decrease in the density of the surrounding electron cloud. Notably, the peak at 285.6 eV related to C—O—R disappears [42]. However, new peaks at 293.4 and 296.2 eV are closely attributed to C—O—$Cl_{3,4}$ and C—$Cl_{3,4}$, respectively [43]. This indicates that the structure of humic acid is subjected to pressure oxidation, leading to the structural derivation of carbon-containing groups and the formation of new groups. In terms of O 1s

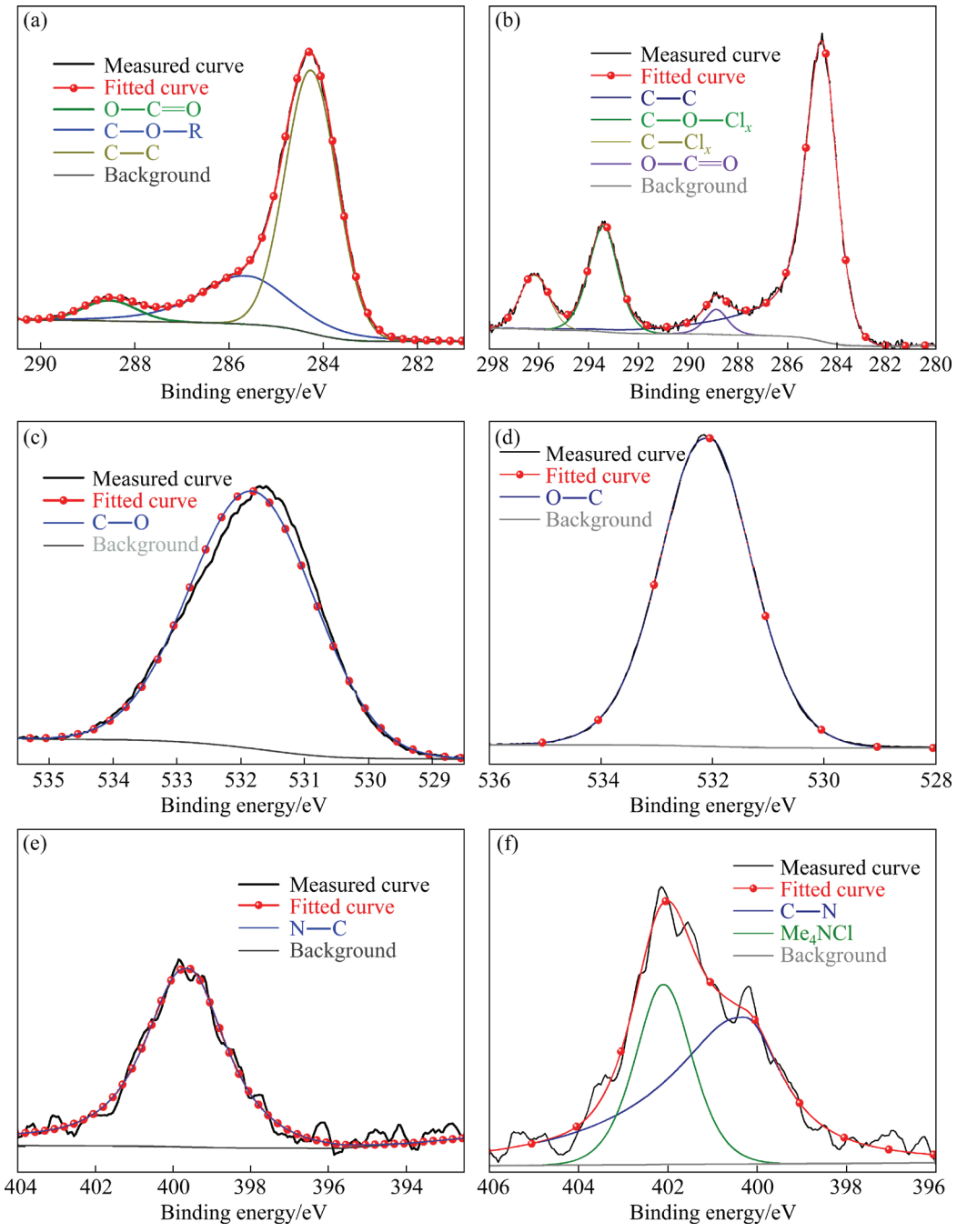

Fig. 6 XPS spectra of C 1s (a, b), O 1s (c, d) and N 1s (e, f) in humic acid from gold concentrate (a, c, e) and pressure-oxidized ore (b, d, f)

spectra, it can be observed that the binding energy of the C—O bond shifts from 531.78 to 532.1 eV, showing that the chemical environment of the C—O bond is affected by pressure oxidation and the density of the electron cloud near the oxygen atom is reduced. According to Fig. 6(f), the N 1s spectra contain a peak at 402.1 eV caused by Me_4NCl [44]. Pressure oxidation decomposes the metal mineral and produces a large number of metal ions. The electronic structure of N in humic acid has changed and the lone pair electrons of N are deflected towards the empty orbital of the metal, generating the coordination. The electron cloud density of the N atom decreases and that of the metal increases, eventually forming a quaternary ammonium structure with Cl stabilized in the humic acid. In addition, a peak at 399.62 eV assigned to the C—N bond is shifted to 400.3 eV [44]. Therefore, the changes in XPS spectra confirm the alternation of the chemical structure of humic acid triggered by pressure oxidation.

3.3 Gold-adsorbing behavior of humic acid

3.3.1 Gold-adsorbing experimental results

Gold-adsorbing experiments of humic acid extracted from pressure-oxidized ore were carried out. The experimental conditions refer to the findings of a previous study [13]. Figure 7(a) depicts the experimental data of humic acid adsorbing pure gold solution. The results show that the adsorption rate of humic acid from gold concentrate is higher that than from pressure-oxidized ore at any pH value. According to our previous study, the maximum adsorption rate was obtained at pH 3.0. The maximum gold-adsorbing rate is (71.50±1.21)% for humic acid from gold concentrate and (42.78±1.05)% for humic acid from pressure-oxidized ore, and the adsorption rate decreases by 40.17%. Similarly, the adsorption experiments of humic acid adsorbing gold leaching solution were conducted under the same conditions, and the results are shown in Fig. 7(b). The adsorption rate reaches (50.98±1.07)% for humic acid from gold concentrate and (28.63±1.11)% for humic acid from pressure-oxidized ore, which decreases by 43.84%. Humic acid from pressure-oxidized ore possesses adsorption capability, and yet the adsorption amount is reduced due to the changes in chemical structure and surface caused by the influence of pressure oxidation.

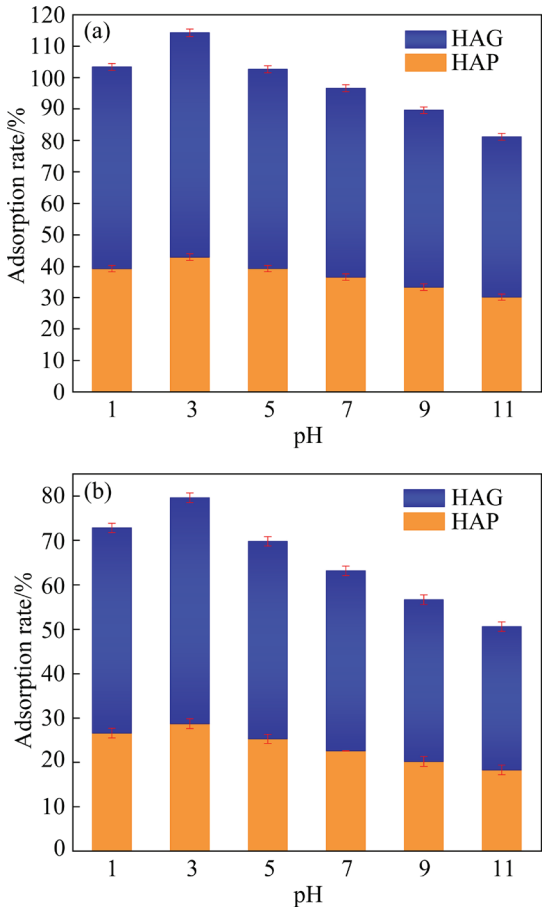

Fig. 7 Change in adsorption rate with different pH: (a) Pure gold solution; (b) Gold leaching solution (HAG−Humic acid extracted from gold concentrate; HAP−Humic acid extracted from pressure-oxidized ore)

3.3.2 Adsorption kinetics and isotherms

Figure 8(a) shows the change curve of adsorption amount with time. The gold adsorption amount of humic acid from pressure-oxidized gold ore gradually increases with the increase in adsorption time. The adsorption amount reaches equilibrium when the adsorption time reaches 7 h. Based on the data in Fig. 8(a), the pseudo-first-order and pseudo-second-order kinetic models of humic acid were established, and the kinetic results are listed in Table 5, Figs. 8(b) and (c). The correlation coefficient R^2 value of the pseudo-first-order is lower than that of the pseudo-second-order, indicating that the pseudo-second-order can describe the gold-adsorbing behavior. Furthermore, the theoretical adsorption amount (22.20 mg/g) calculated from the fitted plot is close to the experimental data (22.16 mg/g). The gold-adsorbing process of humic acid from pressure-oxidized ore is mainly controlled by the rate-limiting step [45],

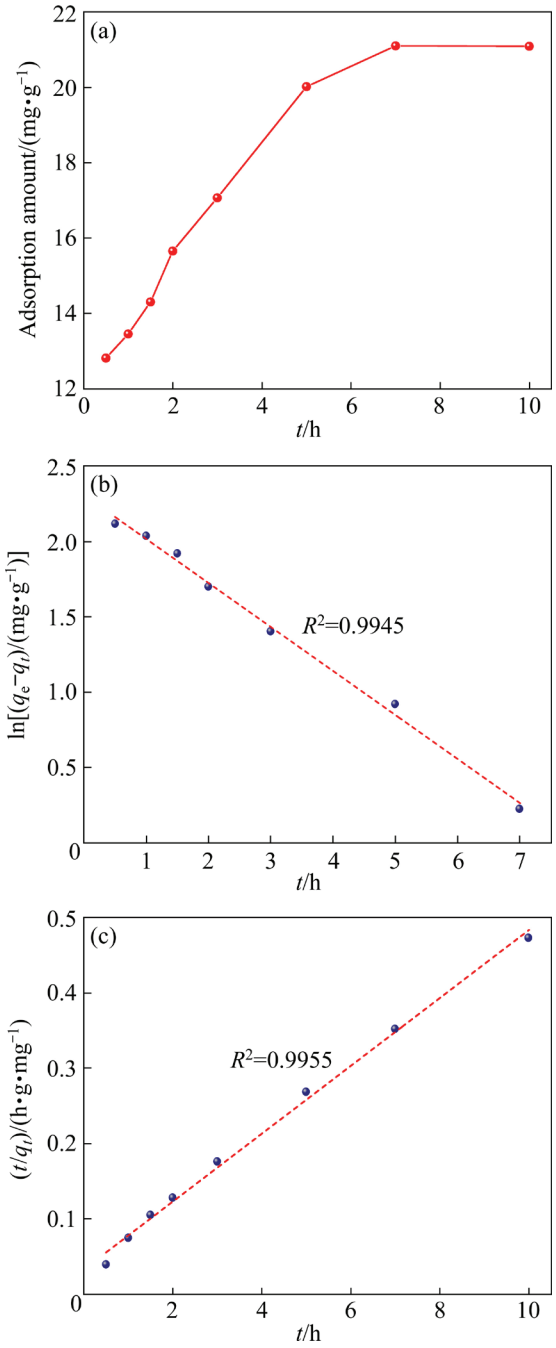

Fig. 8 Change of gold adsorption amount with time (a), and fitting plots of pseudo-first-order (b) and pseudo-second-order (c)

affecting the adsorption capacity. Kinetic analysis shows that the kinetic model of humic acid from pressure-oxidized slag is consistent with that of the gold concentrate.

Figure 9 and Table 6 present the isotherms parameters of the Langmuir and Freundlich models of humic acid from pressure-oxidized ore. It can be found that the R^2 value of the Langmuir model is higher than that of the Freundlich model, showing

Table 5 Kinetic parameters of pseudo-first-order and pseudo-second-order

Pseudo-first-order		
q_e/(mg·g^{-1})	k_1/h^{-1}	R^2
10.08	0.2923	0.9945
Pseudo-second-order		
q_e/(mg·g^{-1})	k_2/(mg·g^{-1}·h^{-1})	R^2
22.20	0.0616	0.9955

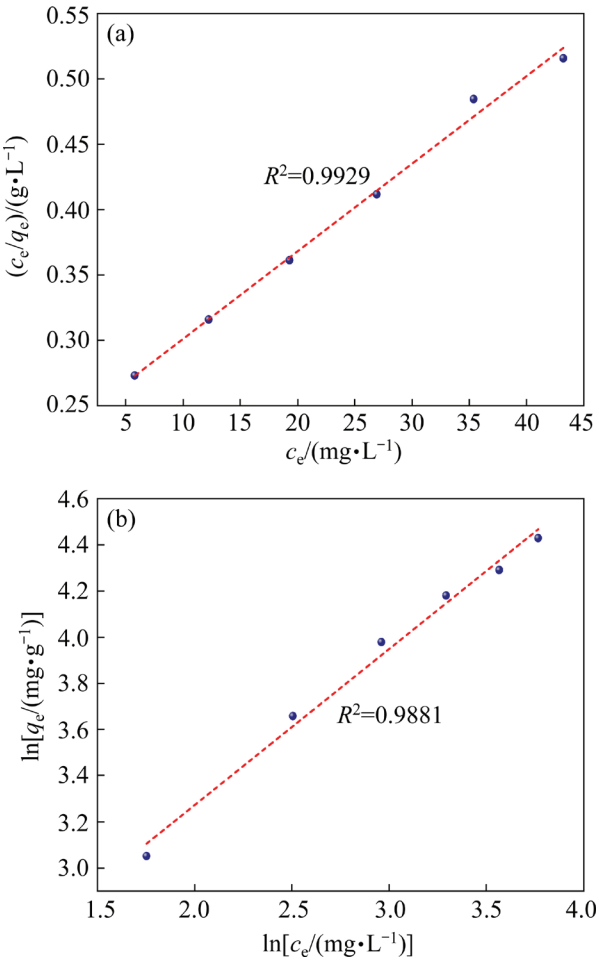

Fig. 9 Fitting plots of Langmuir model (a) and Freundlich model (b)

Table 6 Fitting results of Langmuir and Freundlich models

Langmuir model		
q_m/(mg·g^{-1})	K_L/(L·mg^{-1})	R^2
149.25	0.0286	0.9929
Freundlich model		
n	K_F/(mg·g^{-1}·(mg·L^{-1})$^{-1/n}$)	R^2
1.4776	3.2932	0.9881

that the adsorption process is in accordance with the Langmuir model. This means that the adsorption behavior of humic acid on gold affected by pressure oxidation is monolayer on the homogeneous surface [22]. It differs from the isotherm results of humic acid from gold concentrate. Furthermore, this reveals that pressure oxidation affects humic acid adsorbing gold and the adsorption mechanism.

3.3.3 Thermodynamics and isosteric heat of adsorption

The adsorption thermodynamic parameters, including enthalpy change, entropy change and Gibbs free energy change, were calculated and the results are listed in Table 7. Under different temperatures, $\Delta G < 0$ indicates that the gold-adsorbing of humic acid from pressure-oxidized ore is a spontaneous process. According to $\Delta H > 0$, the gold-adsorbing process is endothermic. Moreover, $\Delta S > 0$ indicates that adsorption is irreversible [46]. However, ΔG, ΔH and ΔS values of humic acid after pressure oxidation are all significantly smaller than those of humic acid extracted from gold concentrate. The main reason for this variation is the profound effect of pressure oxidation on the surface and the chemical structure of humic acid.

The isosteric heat of adsorption at different temperatures was calculated by using Formula (10). Figure 10 shows the fitted plot and Q value variation with the changes in q_e value. From the calculated data, Q value increases with increasing q_e, implying that the surface of humic acid extracted from pressure-oxidized ore is heterogeneous [24]. This is because the number of sites with adsorption capability and chemical structure on the humic acid surface decreases sharply with a gradual increase in adsorption amount, resulting in the surface occupied by the adsorbed gold. Additionally, Q value is lower than the calculated value for humic acid extracted from gold concentrate.

Table 7 Calculated results of adsorption thermodynamic parameters

T/K	ΔH/ (kJ·mol^{-1})	ΔS/ (J·K^{-1}·mol^{-1})	ΔG/ (kJ·mol^{-1})
293	8.14±0.47	88.77±5.03	−17.87±0.93
298	8.47±0.50	89.60±4.97	−18.23±1.01
303	8.91±0.51	91.35±4.98	−18.69±0.98
308	9.15±0.49	91.85±5.01	−19.14±1.05
313	9.22±0.48	92.07±4.98	−19.60±0.96

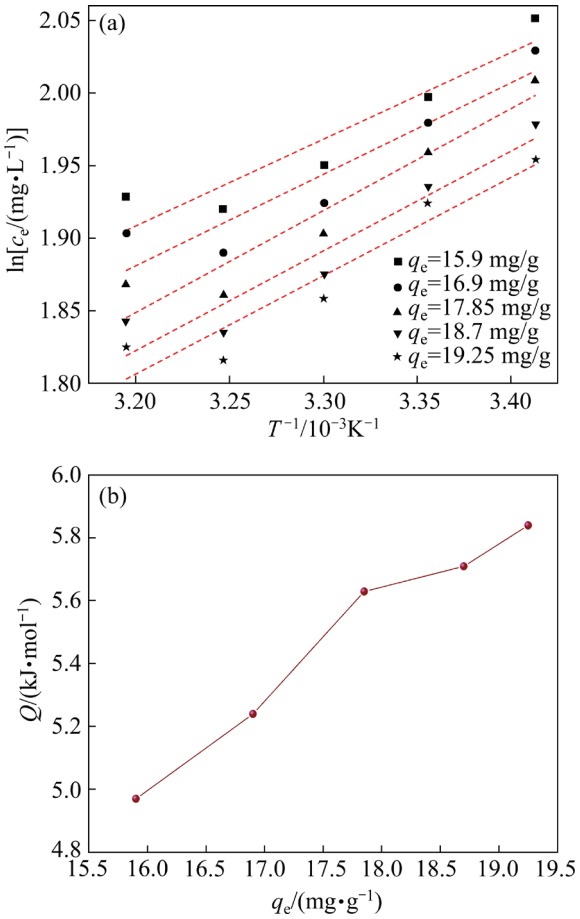

Fig. 10 Plot of ln c_e vs $1/T$ (a) and change in isosteric heat of adsorption (Q) with q_e (b)

4 Conclusions

(1) Under optimal conditions, the yield of humic acid extracted from pressure-oxidized gold ore was (0.9704±0.0008)%, and the extracted amount of humic acid reached 8.26−19.03 mg/g.

(2) Affected by pressure oxidation, aliphatic structures and oxygenated groups were destroyed, carbon surface defects of the extracted humic acid were reduced, and the chemical environment of main elements was changed. Significantly, new structures, such as C—O—Cl$_x$, C—Cl$_x$ and Me$_4$N—Cl, can be observed in the humic acid extracted from pressure-oxidized ore.

(3) The gold-adsorbing experimental results revealed that the adsorption rate of the humic acid extracted from pressure-oxidized gold ore significantly decreased to (42.78±1.05)% for a pure gold solution and (28.63±1.11)% for gold-containing leaching solution at pH 3.0. This suggests that pressure oxidation profoundly impacts the gold-adsorbing capability by changing the

chemical structure and surface activity of humic acid.

(4) In the study of kinetics and isotherms, the adsorption process conformed to the pseudo-second-order kinetic and Langmuir isotherm models. The adsorption process was endothermic and spontaneous, accompanying by an increase in the isosteric heat of adsorption with increasing the equilibrium adsorption amount.

CRediT authorship contribution statement

Hui-qun NIU: Writing − Original draft, Investigation; **Rong-xin ZHAO:** Resources; **Hong-ying YANG:** Funding acquisition; **Lin-lin TONG:** Supervision; **You-qin ZHOU:** Writing – Review & editing.

Declaration of competing interest

The authors declare that they have no known competing financial interests or personal relationships that could have appeared to influence the work reported in this paper.

Acknowledgments

The authors are grateful for the financial support from the National Natural Science Foundation of China (No. 52274348), and the National Key Research & Development Program of China (Nos. 2018YFC1902002, 2018YFC1902001).

References

[1] ZHANG Xin-wei, SONG Yong-hui, WU Lei, DONG Ping, ZHOU Min, LIU Gang. Improvement of the leach efficiency of carbonaceous gold concentrates using reduction roasting pretreatment technology [J]. Advanced Powder Technology, 2022, 33(2): 103387.

[2] SCHMITZ P A, DUYVESTEYN S, JOHNSON W P, ENLOE L, MCMULLEN J. Adsorption of aurocyanide complexes onto carbonaceous matter from preg-robbing Goldstrike ore [J]. Hydrometallurgy, 2001, 61(2): 121−135.

[3] TAN H, FENG D, LUKEY G C, van DEVENTER J. The behavior of carbonaceous matter in cyanide leaching of gold [J]. Hydrometallurgy, 2005, 78(3/4): 226−235.

[4] PYKE B L, JOHNSTON R F, BROOKS P. The characterization and behavior of carbonaceous material in a refractory gold bearing ore [J]. Minerals Engineering, 1999, 12(8): 851−862.

[5] DOSKOCIL L, BURDIKOVA-SZEWIECZKOVA J, ENEV V, KALINA L, WASSERBAUER J. Spectral characterization and comparison of humic acids isolated from some European lignites [J]. Fuel, 2018, 213: 123−132.

[6] LIU Qian, YANG Hong-ying, TONG Lin-lin, JIN Zhe-nan, SAND W. Fungal degradation of elemental carbon in carbonaceous gold ore [J]. Hydrometallurgy, 2016, 160: 90−97.

[7] KALBITZ K, GEYER W, GEYER S. Spectroscopic properties of dissolved humic substances—A reflection of land use history in a fen area [J]. Biogeochemistry, 1999, 47(2): 219−238.

[8] SONG Hai-yan, YIN You-yi, SONG Jian-zhong. The chemical composition and structure of humic acids from different environments [J]. Journal of South China Normal University (Natural Science Edition), 2009, 41(1): 61−66. (in Chinese)

[9] IKEYA K, SLEIGHTER R L, HATCHER P G, WATANABE A. Characterization of the chemical composition of soil humic acids using Fourier transform ion cyclotron resonance mass spectrometry [J]. Geochimica et Cosmochimica Acta, 2015, 153: 169−182.

[10] HUANG Ya-jun, OU Xiao-xia, HU You-biao. Research progress on spectroscopic characterization of humic acids and their mental complexes [J]. Journal of Green Science and Technology, 2016(4): 53−56, 59. (in Chinese)

[11] GIOVANELA M, CRESPO J S, ANTUNES M, ADAMATTI D S, FERNANDES A N, BARISON A, DA SILVA C, GUEGAN R, MOTELICA-HEINO M, SIERRA M. Chemical and spectroscopic characterization of humic acids extracted from the bottom sediments of a Brazilian subtropical micro-basin [J]. Journal of Molecular Structure, 2010, 981(1/2/3): 111−119.

[12] KLUCAKOVA M, VEZNIKOVA K. Micro-organization of humic acids in aqueous solutions [J]. Journal of Molecular Structure, 2017, 1144: 33−40.

[13] NIU Hui-qun, YANG Hong-ying, TONG Lin-lin. Adsorption behaviors of Au(Ⅲ) onto humic acid extracted from gold ore: Adsorptive kinetics, isotherm and mechanism [J]. Colloids and Surfaces A: Physicochemical and Engineering Aspects, 2021, 630: 127442.

[14] NANTHAKUMAR B, PICKLES C A, KELEBEK S. Microwave pretreatment of a double refractory gold ore [J]. Minerals Engineering, 2007, 20(11): 1109−1119.

[15] MUBAROK M Z, WINARKO R, CHAERUN S K, RIZKI I N, ICHLAS Z T. Improving gold recovery from refractory gold ores through biooxidation using iron−sulfur-oxidizing/ sulfur-oxidizing mixotrophic bacteria [J]. Hydrometallurgy, 2016, 168: 69−75.

[16] LI Jun-meng. The current status and development tendency of pretreation process for refractory gold ores [J]. Hydrometallurgy of China, 2003, 22(1): 1−8. (in Chinese)

[17] LAUKKANEN J M, LEPPINEN J O. Application of eMAX analysis of pressure oxidation of refractory gold ores [J]. Minerals Engineering, 1994, 7(2/3): 234−249.

[18] WU J, AHN J, LEE J. Characterization of gold deportment and thiosulfate extraction for a copper-gold concentrate treated by pressure oxidation [J]. Hydrometallurgy, 2022, 207: 105771.

[19] NIU Hui-qun, YANG Hong-ying, TONG Lin-lin. Structural characterization and adsorption capability of carbonaceous matters extracted from carbonaceous gold concentrate [J]. Minerals, 2021, 11(1): 1−17.

[20] DIMOV S S, CHRYSSOULIS S L, SODHI R N. Speciation of surface gold in pressure oxidized carbonaceous gold ores by TOF-SIMS and TOF-LIMS [J]. Applied Surface Science, 2003, 203: 644−647.

[21] QIU Jian-hao, FENG Yi, ZHANG Xiong-fei, JIA Ming-min, YAO Jian-feng. Acid-promoted synthesis of UiO-66 for highly selective adsorption of anionic dyes: Adsorption performance and mechanisms [J]. Journal of Colloid and Interface Science, 2017, 499: 151−158.

[22] ANIRUDHAN T S, RADHAKRISHNAN P G. Thermodynamics and kinetics of adsorption of Cu(II) from aqueous solutions onto a new cation exchanger derived from tamarind fruit shell [J]. Journal of Chemical Thermodynamics, 2008, 40(4): 702−709.

[23] CHOWDHURY S, SAHA P D. Biosorption kinetics, thermodynamics and isosteric heat of sorption of Cu(II) onto tamarindus indica seed powder [J]. Colloids and Surfaces B, 2011, 88(2): 697−705.

[24] SRIVASTAVA V C, MALL I D, MISHRA I M. Adsorption thermodynamics and isosteric heat of adsorption of toxic metal ions onto bagasse fly ash (BFA) and rice husk ash (RHA) [J]. Chemical Engineering Journal, 2007, 132(1/2/3): 267−278.

[25] HUANG Jin-feng, ZHAO Yi-long, ZHAO Jin-xiang, JIAO Ji-feng, LI Tai-yuan. Extraction of humic acid and determination of its component content [J]. Sichuan Animal & Veterinary Sciences, 2007(5): 27−28. (in Chinese)

[26] SEE J H, BRONK D A. Changes in C:N ratios and chemical structures of estuarine humic substances during aging [J]. Marine Chemistry, 2005, 97(3/4): 334−346.

[27] ZHANG Yao-ling, DU Jin-zhou, ZHANG Fen-fen, YU Yi-hua, ZHANG Jing. Chemical characterization of humic substances isolated from mangrove swamp sediments: The Qinglan area of Hainan Island, China [J]. Estuarine Coastal and Shelf Science, 2011, 93(3): 220−227.

[28] POLAK J, SULKOWSKI W, BARTOSZEK M, PAPIEZ W. Spectroscopic studies of the progress of humification processes in humic acid extracted from sewage sludge [J]. Journal of Molecular Structure, 2004, 744: 983−989.

[29] CHEN J, GU B H, LEBOEUF E J, PAN H J, DAI S. Spectroscopic characterization of the structural and functional properties of natural organic matter fractions [J]. Chemosphere, 2002, 48(1): 59−68.

[30] AMIR S, JOURAIPHY A, MEDDICH A, EL GHAROUS M, WINTERTON P, HAFIDI M. Structural study of humic acids during composting of activated sludge-green waste: Elemental analysis, FTIR and ^{13}C NMR [J]. Journal of Hazardous Materials, 2010, 177(1/2/3): 524−529.

[31] DROBNIAK A, MASTALERZ M. Chemical evolution of Miocene wood: Example from the Belchatow brown coal deposit, central Poland [J]. International Journal of Coal Geology, 2005, 66(3): 157−178.

[32] YANG Hai-ping, YAN Rong, CHEN Han-ping, LEE Dong-ho, ZHENG Chun-guang. Characteristics of hemicellulose, cellulose and lignin pyrolysis [J]. Fuel, 2007, 86(12): 1781−1788.

[33] ARANGANATHAN L, RAJASREE S R, SUMAN T Y, REMYA R R, GAYATHRI S, JAYASEELAN C, KARTHIH M G, GOBALAKRISHNAN M. Comparison of molecular characteristics of Type A humic acids derived from fish waste and sugarcane bagasse co-compost influenced by various alkaline extraction protocols [J]. Microchemical Journal, 2019, 149: 104038.

[34] HANC A, ENEV V, HREBECKOVA T, KLUCAKOVA M, PEKAR M. Characterization of humic acids in a continuous-feeding vermicomposting system with horse manure[J]. Waste Management, 2019, 99: 1−11.

[35] LIU Feng-lei, PENG Gui-long, LI Tong, YU Gang, DENG Shu-bo. Au(III) adsorption and reduction to gold particles on cost-effective tannin acid immobilized dialdehyde corn starch [J]. Chemical Engineering Journal, 2019, 370: 228−236.

[36] LIPSKI M, SLAWINSKI J, ZYCH D. Changes in the luminescent properties of humic acids induced by UV radiation [J]. Journal of Fluorescence, 1999, 9(2): 133−138.

[37] HUCULAK-MACZKA M, HOFFMANN J, HOFFMANN K. Evaluation of the possibilities of using humic acids obtained from lignite in the production of commercial fertilizers [J]. Journal of Soils and Sediments, 2018, 18(8): 2868−2880.

[38] HU S Y, EVANS K, CRAW D, REMPEL K, BOURDET J, DICK J, GRICE K. Raman characterization of carbonaceous material in the Macraes orogenic gold deposit and metasedimentary host rocks, New Zealand [J]. Ore Geology Reviews, 2015, 70: 80−95.

[39] SHARMA S, RODEMANN T, DAVIDSON G. Raman spectroscopy enables the classification of molybdenite phases in the presence of carbonaceous material from Merlin Mo−Re deposit, Australia [J]. Vibrational Spectroscopy, 2016, 86: 8−13.

[40] CUESTA A, DHAMELINCOURT P, LAUREYNS J, MARTINEZ-ALONSO A, TASCON J. Comparative performance of X-ray diffraction and Raman microprobe techniques for the study of carbon materials [J]. Journal of Materials Chemistry, 1998, 8(12): 2875−2879.

[41] ESHKENAZI V, PELED E, BURSTEIN L, GOLODNITSKY D. XPS analysis of the SEI formed on carbonaceous materials [J]. Solid State Ionics, 2004, 170(1/2): 83−91.

[42] ZHANG N N, EJTEMAEI M, NGUYEN A V, ZHOU C C. XPS analysis of the surface chemistry of sulfuric acid-treated kaolinite and diaspore minerals with flotation reagents [J]. Minerals Engineering, 2019, 136: 1−7.

[43] DUAN Xin-ping, YIN Yan, TIAN Xue-lin, KE Jin-huo, WEN Zhao-jun, ZHENG Jian-wei, HU Meng-lin, YE Lin-min, YUAN You-zhu. C−X (X=Cl, Br, I) bond dissociation energy as a descriptor for the redispersion of sintered Au/AC catalysts [J]. Chinese Journal of Catalysis, 2016, 37(10): 1794−1803.

[44] SHI Zhan-ming, YE Xin-yue, LIANG Kai-ming, GU Shu-rui, PAN Fei. XPS analysis of light elements (C, N) remaining in sol−gel derived TiO_2 films [J]. Journal of Materials Science Letters, 2003, 22(18): 1255−1258.

[45] HO Y S, MCKAY G. Pseudo-second order model for sorption processes [J]. Process Biochemistry, 1999, 34(5): 451−465.

[46] GUERRA D, MELLO I, RESENDE R, SILVA R. Kinetics and thermodynamics of Cr(VI) ion adsorption onto organo-bentonite from the Amazon region [J]. Reaction Kinetics, Mechanisms and Catalysis, 2013, 108(2): 317−339.

加压氧化过程中胡敏酸结构和吸附特性的变化

牛会群[1,2]，赵荣欣[3]，杨洪英[1,2]，佟琳琳[1,2]，周有勤[2,4]

1. 东北大学 多金属共生矿生态化冶金教育部重点实验室，沈阳 110819；
2. 东北大学 冶金学院，沈阳 110819；
3. 山东黄金集团 焦家金矿，莱州 264100；
4. Joe Zhou Mineralogy Ltd., Peterborough, Ontario K9L 2A6, Canada

摘　要：从碳质加压氧化金矿中提取胡敏酸。采用元素分析、傅里叶转换红外光谱、紫外−可见光光谱、拉曼光谱和 X 射线光电子能谱分析胡敏酸的结构。建立胡敏酸吸附金的动力学和等温线模型，计算热力学参数和等量吸附热。结果表明，受加压氧化的影响，胡敏酸的脂肪族结构、C═O 键及其他含氧基团被破坏。更重要地，胡敏酸结构中有新化学键形成，如 C—O—Cl_x、C—Cl_x 和 Me_4N—Cl。吸附实验结果显示，加压氧化对胡敏酸的金吸附性能具有极大影响。加压氧化后，胡敏酸对纯金溶液的吸附率下降至(42.78±1.05)%，对金浸出液的吸附率下降至(28.63±1.11)%。吸附数据表明，胡敏酸对金吸附行为符合伪二级动力学和 Langmuir 等温线模型。胡敏酸的等量吸附热随吸附量的增加而增加。

关键词：胡敏酸；正交实验；加压氧化；结构变化；吸附行为

(Edited by Wei-ping CHEN)